Ni-Pt Phase Diagram: Experiment and Theory

C. E. Dahmani and M. C. Cadeville
Laboratoire de Magnétisme et de Structure Electronique des Solides, Université Louis Pasteur, 67070 Strasbourg Cedex, France

and

J. M. Sanchez
Henry Krumb School of Mines, Columbia University, New York, New York 10027

and

J. L. Morán-López
Departamento de Física, Centro de Investigación y de Estudios Avanzados del Instituto Politécnico Nacional, 07000 México, D. F., Mexico

(Received 22 July 1985)

The temperature-composition phase diagram of the $Ni_{1-x}Pt_x$ system was determined by x-ray diffraction and *in situ* high-temperature measurements of electrical resistivity. The Curie temperatures were also determined for both disordered and ordered alloys. Our results provide direct experimental evidence for the interplay between atomic ordering and magnetism. The experimental measurements are satisfactorily reproduced by a Hamiltonian, solved in the tetrahedron approximation of the cluster-variation method, that contains magnetic interactions dependent on chemical and short-range order.

PACS numbers: 75.30.Kz, 75.10.Hk, 75.50.Cc, 81.40.Rs

The nature of chemical and magnetic interactions in solid solutions, their interdependence, and the role that these interactions play in determining the phase diagram of transition-metal alloys has recently received increased attention from experimentalists[1-5] and theoreticians.[6-8] Despite such efforts, however, the current understanding of the interplay between magnetic and chemical ordering in alloys is less than satisfactory. In fact, with the exception of very recent work,[4,5] most experimental phase equilibrium studies in magnetic alloys are focused on either the chemical or the magnetic interactions separately, rather than on their combined effect. Thus, the evidence for the interdependence between magnetic and chemical order is mostly indirect and based strictly on the interpretation of experimental results via theoretical models.[2] Moreover, the theoretical models themselves, which are commonly based on the molecular-field, the Bragg-Williams, or the quasichemical approximation, are known to be very inaccurate for nonmagnetic fcc ordering alloys.[9] Consequently, such models cannot be expected to describe reliably the more complicated case of magnetic fcc alloys. For these systems, significantly improved results can be obtained by use of other mean-field theories such as the tetrahedron approximation of the cluster-variation method. Only recently, however, have these high-order cluster approximations been used to investigate phase equilibrium in magnetic alloys.[7] The main purpose of this investigation is to study the interplay between atomic ordering and magnetic behavior experimentally, by determining the magnetic transition in alloys with different degrees of short- and long-range order, and theoretically, by modeling stable and metastable equilibrium via the cluster-variation method.

The alloy chosen for the present study is the binary Ni-Pt system. In this Letter we report a detailed determination of the chemical and magnetic phase diagram along with a cluster-variation calculation of phase equilibrium in the full temperature-composition range. Our experimental results clearly show the importance of chemical long- and short-range order for the magnetic properties of alloys. Furthermore, we also show that the experimental results can be accurately explained by a simple model Hamiltonian, solved by use of the tetrahedron approximation, that includes chemical and magnetic interactions.

The Ni-Pt phase diagram is relatively simple. At high temperatures, the paramagnetic fcc solid solution ($A1$) is stable in the whole range of concentrations. At intermediate temperatures, these disordered solid solutions transform via first-order transitions to paramagnetic ordered phases: $L1_2$ (Ni_3Pt) or $L1_0$ (NiPt).[10] An ordered $NiPt_3$ phase ($L1_2$), with a congruent temperature slightly lower than that of the Ni_3Pt phase, has also been reported.[11] Finally, at low temperatures and for atomic concentrations of Pt below 0.6, the $A1$ and the Ni_3Pt phases transform to a ferromagnetic state.

The order-disorder transition and the Curie temperatures were determined for several alloys with Pt atomic concentrations between 0 and 0.6. The Curie temperatures were measured for both disordered and ordered phases. As discussed elsewhere, determina-

tion of the *equilibrium* transus lines requires a rather detailed characterization of the kinetics of order-disorder.[12] Such kinetic analysis has been carried out for the $A1$, $L1_2$, and $L1_0$ phases in the Ni-Pt system,[12] and it is used here to determine portions of the equilibrium phase diagram by high-temperature measurements of electrical resistivity. We start from a well-defined equilibrium state at low temperatures, obtained after a long-time annealing and characterized by x-ray diffraction. The temperature derivative of the equilibrium electrical resistivity, which is a very sensitive function of short- and long-range order, is then investigated as a function of temperature. In general, this allows for an accurate determination of the temperature T_{c1} at which the first disordered domain nucleates, and of the temperature T_{c2} at which the disordering reaction is completed. This technique, although very accurate, is limited to a temperature region where equilibrium can be attained in a reasonably short period of time (in our case less than a month, which corresponds to a lower temperature limit of approximately 700 K). For lower temperatures, the order-disorder transus lines were obtained by use of conventional x-ray techniques, i.e., samples annealed at high temperatures were quenched to room temperature and the phases present determined by x-ray diffraction. For further details on the sample preparation and on the resistivity measurements the reader is referred to Ref. 4.

Our experimental results for the order-disorder transition temperatures are shown in Fig. 1. T_{c1} and T_{c2} correspond respectively to the solubility limits of the disordered and ordered phases as determined from the resistivity measurements. The remaining symbols in Fig. 1 indicate the results of the x-ray diffraction experiments. Coexistence of the disordered phase $A1$ with the ordered $L1_2$ and $L1_0$ phases is shown respectively by solid circles and solid squares. The open circles and open squares indicate single-phase regions in the diagram for, respectively, the Ni_3Pt and the NiPt phases. The solid lines are our theoretical results, which are described below.

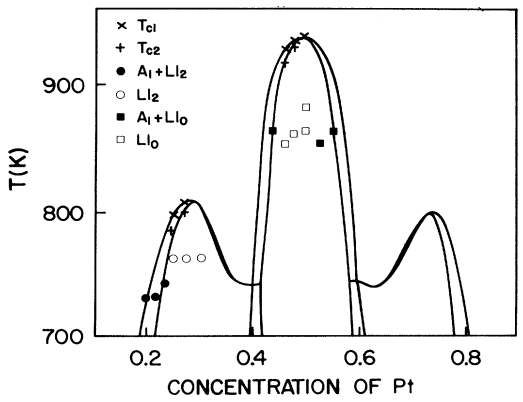

FIG. 1. The high-temperature phase diagram of $Ni_{1-x}Pt_x$. The phases observed experimentally are marked by squares and circles. The results of the calculations are the solid lines.

The concentration dependence of the Curie temperature is shown in Fig. 2 for disordered alloys quenched from high-temperature equilibrium states (open circles) and for ordered alloys annealed at approximately 700 K, where equilibrium states could be attained (crosses). The dotted and dashed lines are the calculated Curie temperature T_m obtained by freezing of the atomic order at 2000 and 730 K, respectively.

It is well established[13,14] that the tetrahedron is the lowest mean-field approximation that can reproduce the topology of the order-disorder phase diagram observed in several fcc-based alloys. Lower mean-field approximations, such as Bragg-Williams, fail to reproduce the first-order character of the transition at the AB stoichiometry as well as the three observed maxima (congruent points) near the stoichiometric compositions AB_3, AB, and A_3B. Thus, we adopt a tetrahedron as the unit in the cluster-variation calculation.

We model the $Ni_{1-x}Pt_x$ alloy by a binary system $A_{1-x}B_x$ with one magnetic component A. The atomic species and the magnetic moment at a given lattice site i are characterized respectively by a chemical occupation operator σ_i and by a spin operator s_i. The occupation operator σ_i equals 1 for A atoms and -1 for B

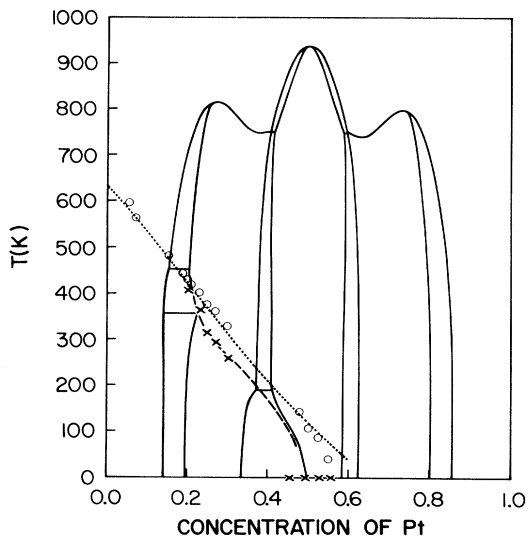

FIG. 2. The low-temperature phase diagram of $Ni_{1-x}Pt_x$. The experimental results are marked by circles and crosses. The results of the calculation for alloys with frozen atomic order at 2000 and 730 K are shown by dotted and dashed lines, respectively.

atoms. We restrict ourselves to the case where the spin of the A component is $\frac{1}{2}$. To simulate the well-known environmental effects on the Ni magnetic moment, we assume that the exchange interactions between two nearest-neighbor Ni atoms vanish unless a third Ni atom is also present as a common nearest neighbor to the other two. In reality, the magnetic interactions in the Ni-Pt system are apparently more complex: A recent study carried out by two of the present authors indicates that the magnetic moment on Ni atoms depends not only on the local environment (short-range order), but also on long-range order and on the alloy average concentration.[4,5]

In what follows, we adopt a Hamiltonian that contains both chemical and magnetic interactions:

$$H = H_{\text{chem}} + H_{\text{mag}}. \tag{1}$$

If we take into account many-particle interactions, the chemical contribution to the energy can be written as

$$H_{\text{chem}} = V_2 \sum_{ij} \sigma_i \sigma_j + V_3 \sum_{ijk} \sigma_i \sigma_j \sigma_k + V_4 \sum_{ijkl} \sigma_i \sigma_j \sigma_k \sigma_l, \tag{2}$$

where V_2, V_3, and V_4 are effective interactions between two, three, and four atoms, respectively, and where the sums in Eq. (2) are carried out over all nearest-neighbor pairs, triangles, and tetrahedra in the lattice. The three- and four-body interactions are included in order to model the asymmetry with respect to concentration in the order-disorder phase boundaries.[14]

In the absence of magnetic fields, the magnetic energy contribution is of the form

$$H_{\text{mag}} = \sum_{ijkl} J_{i(kl)j} s_i s_j, \tag{3}$$

where the sum is carried out over all tetrahedron clusters in the lattice. In Eq. (3), the exchange integral $J_{i(kl)j}$ between nearest-neighbor Ni atoms at sites i and j depends on the occupancy of the nearest-neighbor sites k and l. We assume that the exchange interactions J are nonzero only in the event that at least one of the nearest-neighbor sites k or l is also occupied by a Ni atom. A set of Hamiltonian parameters that reproduce accurately the Ni-Pt phase diagram is $V_2 = 458.43k = 907.7$ cal/mole, $V_3 = 0.003 V_2$, $V_4 = -0.05 V_2$, $J_{\text{Ni(NiNi)Ni}} = -0.1373 V_2$, and $J_{\text{Ni(NiPt)Ni}} = -0.1 V_2$.

The equilibrium phase diagram obtained by minimization of the free energy with the parameters given above is shown in Fig. 3. The high-temperature region shows the typical three maxima around the stoichiometric compositions AB_3, AB, and A_3B. In Fig. 1 we compare the theoretical results with the measurements. As a result of the many-body interactions,

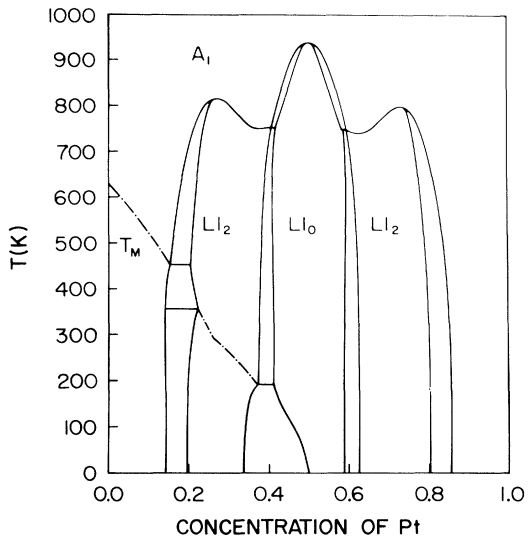

FIG. 3. The calculated equilibrium phase diagram of $Ni_{1-x}Pt_x$ obtained with the parameters $V_2 = 907.7$ cal/mole, $V_3 = 0.003 V_2$, $V_4 = -0.05 V_2$, $J_{\text{Ni(NiNi)Ni}} = -0.1373 V_2$, and $J_{\text{Ni(NiPt)Ni}} = -0.1 V_2$.

the phase diagram is asymmetric. This effect, included here for completeness, is very small and it can be ignored in a first approximation.

The most interesting behavior is seen to occur at low temperatures, where the system becomes ferromagnetic. For low Pt concentrations, a wider two-phase region is observed between critical end points, with the latter indicated by horizontal lines in Fig. 3. In this region, the ferromagnetic disordered solid solution ($A1$) coexists with a paramagnetic $L1_2$ ordered phase (Ni_3Pt). The width of the two-phase region decreases again at lower temperatures, where the coexisting phases are both ferromagnetic.

The effect of magnetic interactions on the equilibrium phase diagram is considerably more pronounced for Pt concentrations near 0.4. Here, the ferromagnetic Ni_3Pt and the paramagnetic NiPt phases coexist. The predicted two-phase boundaries cannot be confirmed experimentally, however, because of the slowness of diffusion at such low temperatures. We see from Fig. 3 that, in the NiPt ($L1_0$) structure, the ferromagnetic state is completely suppressed by chemical long-range order. Within our model, this is due to the vanishing of the magnetic moment on Ni atoms near AB stoichiometry at low temperatures which, in turn, follows from the fact that the perfectly ordered $L1_0$ structure does not have rings of three or more nearest-neighbor Ni atoms.

To study the effect of atomic ordering on magnetic properties, and to compare with the experimental results, we have calculated the Curie temperature of

quenched alloys. In these calculations, the free energy is minimized with respect to the magnetic degrees of freedom while chemical short- and/or long-range order (up to the tetrahedron level) is frozen at a higher temperature. The results of the calculations for systems quenched from 2000 and 730 K are shown and compared with our experimental measurements in Fig. 2. We see from this figure that the theory is in excellent agreement with experiment, particularly for the $A1$ and $L1_2$ phases. Small discrepancies are seen for Pt concentrations in the neighborhood of 0.5. For the disordered alloys, the observed percolation limit, at which the magnetic state disappears at zero temperature, seems to be slightly lower than predicted by the theory although, in part, the discrepancy may be due to the fact that the perfect quenching achieved in the calculations is not experimentally attainable. For ordered alloys, the experimental observation concerning the disappearance of magnetism in the $L1_0$ phase is in better agreement with the calculations for the equilibrium system (shown in Fig. 3) than with the calculations for ordered alloys quenched from approximately 700 K.

In conclusion, (i) we have reported the most complete phase diagram for the Ni-Pt system; (ii) the interplay between atomic ordering and magnetism has been clearly established; (iii) the experimental results have been accurately reproduced by solving a Hamiltonian that contains chemical and magnetic contributions in the tetrahedron approximation of the cluster-variation method; and (iv) the calculations predict pronounced effects on the equilibrium phase diagram particularly when the phases involved are of mixed magnetic character.

This work was supported in the U. S. by the National Science Foundation through Grant No. DMR-8206195 and No. INT-8409776, and in Mexico by Consejo Nacional de Ciencia y Tecnología through Grant No. PCCBBEU-022007 and by Consejo del Sistema Nacional de Educación Tecnológica de la Secretaria de Educación Pública.

[1]J. K. van Deen and F. van der Woude, Acta Metall. **29**, 1255 (1981).

[2]A. P. Miodownik, Bull. Alloy Phase Diagrams **2**, 406 (1982).

[3]V. Pierron-Bohnes, M. C. Cadeville, and F. Gautier, J. Phys. F **13**, 1689 (1983).

[4]C. E. Dahmani, Thesis, Université Louis Pasteur, 1985 (unpublished).

[5]M. C. Cadeville, C. E. Dahmani, and F. Kern, to be published.

[6]R. A. Tahir-Kheli and T. Kawasaki, J. Phys. C **10**, 2207 (1977).

[7]J. M. Sanchez and C. H. Lin, Phys. Rev. B **30**, 1448 (1984).

[8]F. J. Martinez-Herrera, F. Mejía-Lira, F. Aguilera-Granja, and J. L. Morán-López, Phys. Rev. B **31**, 1686 (1985).

[9]J. M. Sanchez, D. de Fontaine, and W. Teitler, Phys. Rev. B **26**, 1465 (1982).

[10]M. Hensen, *Constitution of Binary Alloys* (McGraw Hill, New York, 1958), 2nd Ed.

[11]G. Inden, private communication.

[12]C. E. Dahmani, M. C. Cadeville, and V. Pierron-Bohnes, Acta Metall. **33**, 369 (1985).

[13]C. M. van Baal, Physica (Utrecht) **64**, 571 (1973).

[14]D. de Fontaine and R. Kikuchi, in *Applications of Phase Diagrams in Metallurgy and Ceramics,* edited by C. G. Carger, U. S. National Bureau of Standards Special Publication No. 496 (U. S. Government Printing Office, Washington, D. C., 1978), p. 917.